- Technical Paper -

INFLUENCE OF COEXISTING GEOPOLYMERIZATION AND CEMENT HYDRATION ON DRYING SHRINKAGE BEHAVIOR OF CEMENT-ADDED FLY ASH-BASED GEOPOLYMER MORTAR

Horhok LIM[*1], Mitsuyasu IWANAMI[*2] and Kazuhide NAKAYAMA[*3]

ABSTRACT

Evaporation of water generated during dehydration is one of the key factors in the drying shrinkage of geopolymer. This study examined the coexistence of geopolymer and cement to evaluate its influence on drying shrinkage of geopolymer. Fly ash was partially replaced with 10% cement with the aim of consuming pore water through hydration to suppress water evaporation and reduce drying shrinkage. Cement hydration was accelerated due to the high alkalinity of geopolymer solution, which adversely altered the reaction products and pore structures of geopolymer, resulting in larger drying shrinkage.

Keywords: geopolymer, drying shrinkage, dehydration, cement addition, hydration

1. INTRODUCTION

Geopolymer hardens through a dehydration polycondensation reaction between an alkaline solution and an activated filler, such as fly ash, which is an industrial byproduct. Moreover, geopolymer demonstrates remarkable properties, such as high resistance to fire, acid, alkali silica reaction, along with the ability to immobilize heavy metals and radioactive substances [1,2]. However, during dehydration of geopolymer, water is produced within the hardened matrix. The evaporation of this water is considered to lead to significant drying shrinkage [3], which can adversely affect the material's mechanical properties and durability [4]. Given the nature of cement hydration reaction, the presence of cement in geopolymer may act as a water absorbent. Therefore, this study hypothesized that a partial incorporation of cement into the geopolymer matrix could reduce drying shrinkage by immobilizing water through hydration. In addition to its ability to absorb water, reaction products of cement could reduce the porosity, leading to the improvement of the material strength and mass transfer resistance.

Hereinafter, "geopolymer" is referred to as a material that hardens mainly by dehydration polycondensation and partially by hydration when is subjected to cement addition, similar to fly ash-blast furnace slag based geopolymer which contains both geopolymerization and hydration products due to the existence of calcium [4].

This study aimed to examine the influence of cement incorporation on drying shrinkage behavior of fly ash-based geopolymer mortar by replacing a small portion of fly ash with cement, with a particular focus on the coexistence of geopolymerization and hydration. Changes in length and mass loss of the cement-added geopolymer mortar were measured to assess the drying shrinkage strain and its correlation with the degree of water evaporation. In addition to compression test, scanning electron microscope (SEM) and X-ray diffraction (XRD) were employed to inspect the reaction product structures, while mercury intrusion porosimetry (MIP) was used to analyze the pore size distribution.

2. EXPERIMENTAL PROGRAMS

2.1 Materials and Mix Proportions

Table 1 presents the mix proportions of the specimens. Fly ash (FA, Type II) was used as an activated filler to better visualize the reaction mechanism when cement is mixed with geopolymer materials, as the main reaction of fly ash-based geopolymer is dehydration polycondensation. Ordinary Portland cement (OPC) was used to partially replace FA

Table 1 Mix proportions

W	Si/A	L/P	Specimen name	OPC replacement ratio (%)	Unit weight (g/L)						
					Cement paste		Geopolymer mortar				
							Activated filler	Alkaline solution			Sand
					OPC	Water	FA	SS	SH solution		
									SH	Water	
0.125	0.700	1	OPC0	0	0	0	579.0	167.5	20.91	136.1	1350
			OPC10	10	59.40	32.66	534.5	167.5	20.91	103.4	1350

*1 Dept. of Civil and Environmental Engineering, Institute of Science Tokyo, JCI Student Member
*2 Prof., Dept. of Civil and Environmental Engineering, Institute of Science Tokyo, Dr.E., JCI Member
*3 Assistant Prof., Dept. of Civil and Environmental Engineering, Institute of Science Tokyo, Dr.E., JCI Member

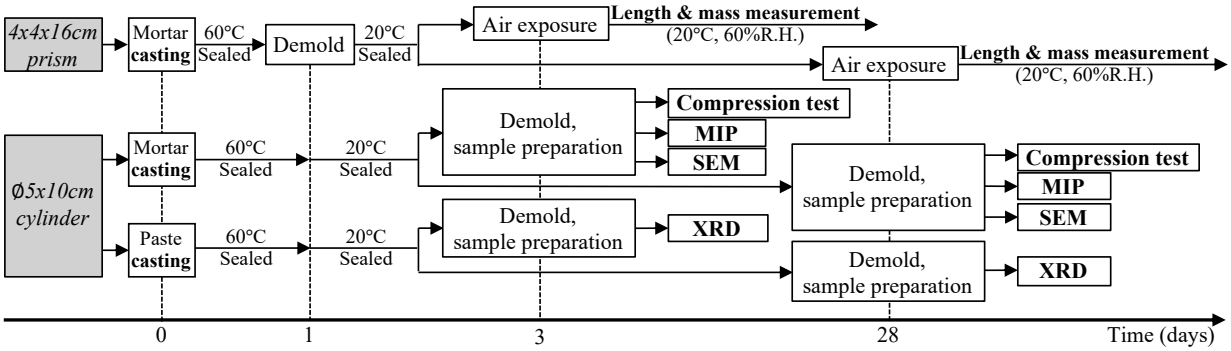

Fig. 1 Experimental flow

Table 2 Material properties

		FA	OPC
Density (g/cm^3)		2.37	3.16
Specific surface area (cm^2/g)		3930	3390
Chemical composition (%)	CaO	4.52	64.23
	Al_2O_3	22.04	5.52
	SiO_2	59.81	21.42

at replacement ratios of 0% and 10% by volume. The replacement ratio was determined balancing the workability based on preliminary experiment, the scale of the effect, and the environmental impact, without overusing OPC which compromises the concept of geopolymer. The alkaline solution was prepared by mixing sodium silicate solution (SS, water glass No.1 specified in JIS K 1408), sodium hydroxide (SH), and water. Material properties are presented in Table 2. The mix proportions were designed based on the mix proportion proposed in the common test organized by the Japan Society of Civil Engineers (JSCE), with an alkaline-to-water molar ratio (A/W), silica-to-alkaline molar ratio (Si/A), and liquid-to-powder ratio (L/P) of 0.125, 0.700, and 1, respectively [4]. The standard sand supplied by the Japan Cement Association was used.

2.2 Casting and Curing

The alkaline solution was prepared and stored at room temperature one day prior to casting. For OPC0, fly ash was mixed with the alkaline solution for 30 seconds before mixing with sand for 90 seconds, to make geopolymer mortar. For OPC10, cement replacement was carried out by preparing cement paste separately 30 minutes in advance. This is because it has been reported that an increase in alkali content in a fresh cementitious mixture promotes setting and decreases workability due to the accelerated hydration of C_3A [5]. Therefore, in doing so, it allows C_3A hydration to sufficiently take place beforehand. The water used for the cement paste was allocated from the water in the alkaline solution to maintain the water content across in the entire mixture. Geopolymer mortar was prepared concurrently to ensure it was ready when the cement paste reached the required 30 minutes of resting time. Subsequently, the cement paste was mixed with the geopolymer mortar.

The final mixture was cast into either 4x4x16cm prismatic molds or ø5x10cm cylindrical molds, depending on the type of test, as described in Fig. 1. The surface of the molds was covered with plastic and wrapped with aluminum tape. All specimens underwent sealed heated curing at 60ºC for the first 24 hours, followed by curing at 20ºC for the remainder of the curing periods, which were set at 3 days and 28 days.

2.3 Test Items

Fig. 1 depicts the experimental flow for each test including the specimen preparation.

(1) Change of length and mass loss test

The change of length test was performed in accordance with JIS A 1129-2, measuring the change in length of the specimens over time using a contact gauge, to evaluate drying shrinkage. Gauge plugs were attached to two sides (except the bottom and cast surface) of 4x4x16cm molds before casting. After 24 hours of sealed heated curing, the specimens were demolded, wrapped in plastic and aluminum tape to maintain sealed curing, and then stored at 20ºC. After 3 or 28 days, the specimens (see Fig. 2) were exposed to a 20ºC and 60% relative humidity (R.H.) environment, marking the beginning of the change of length and mass loss tests. Three specimens were prepared for each condition to ensure consistency and reliability.

(2) Compression test

ø5x10cm cylindrical specimens were demolded after 3 or 28 days of sealed curing and had their surfaces polished approximately two hours before the compression test. The test was conducted in accordance with JIS A 1108.

(3) Pore size distribution analysis by mercury intrusion porosimetry (MIP)

MIP was employed to analyze the pore size distribution of the reaction products, providing insights into the drying shrinkage behavior. Samples for MIP were prepared by crushing the ø5x10cm cylindrical specimens into fragments measuring 2.5~5mm. To halt the hardening process, the samples were immersed in acetone for 24 hours, with deaeration applied during the first hour to facilitate the immersion. The samples were then subjected to two consecutive 15-minute ultrasonic

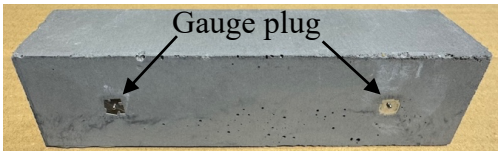

Fig. 2 Specimen for change of length test

baths, followed by additional hour of deaeration. Afterwards, the samples were dried in a 40ºC oven for at least one day before analysis.

(4) Microstructure observation by scanning electron microscope (SEM)

SEM was utilized to observe the microstructure of the reaction products in order to examine the transformation of geopolymer in the presence of cement, as well as the cement hydration products themselves. The samples for the observation were prepared in the same manner as the MIP samples, except that the samples were crushed to an approximate 5x5mm cross-sectional size, with a maximum height of 7mm.

(5) X-ray diffraction analysis

XRD analysis was carried out to identify the crystalline hydration products in the reaction products and quantify their amount. Unlike other tests whose specimens were mortar, samples for XRD were made from paste to facilitate the sample preparation and simplify the analysis. Additional XRD analysis was conducted on cement paste prepared with the alkaline solution to identify the reaction products and compare them with those of OPC0 and OPC10.

3. RESULTS AND DISCUSSIONS

3.1 Coexistence of Geopolymerization and Cement Hydration

Fig. 3 shows the average compressive strength at each OPC replacement ratio under each curing period. With the addition of cement, the compressive strength decreased by 28.4% and 28.9% after 3 and 28 days of curing, respectively. This suggests that the presence of cement interferes with the geopolymerization process, resulting in lower strength development of the geopolymer mortar.

Fig. 4 displays the microstructure of the geopolymer mortar cured for 28 days, as observed by SEM. The reaction products of geopolymer without OPC appear in the form of columnar structure. For OPC10, despite the addition of cement, typical cement hydration products, such as calcium silicate hydrate (C-S-H), calcium hydroxide ($Ca(OH)_2$), and ettringite were unnoticeable. Moreover, the columnar structure resembling geopolymer gel apparently became finer and nearly disappeared.

Phair et al. reported that, under high alkalinity, the precipitation of $Ca(OH)_2$ suppresses calcium solubility, preventing its participation in hydration to form C-S-H [6]. Given that the pH of the alkaline solution in geopolymer used in this study was higher than 14 (6.95 M NaOH), the precipitation of $Ca(OH)_2$ occurs rapidly upon cement addition, resulting in the absence of C-S-H

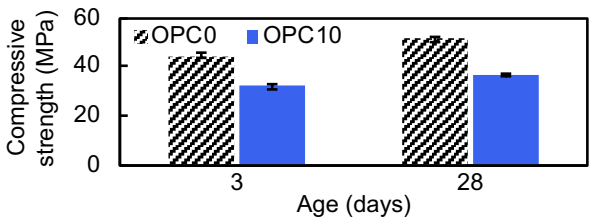

Fig. 3 Compressive strength

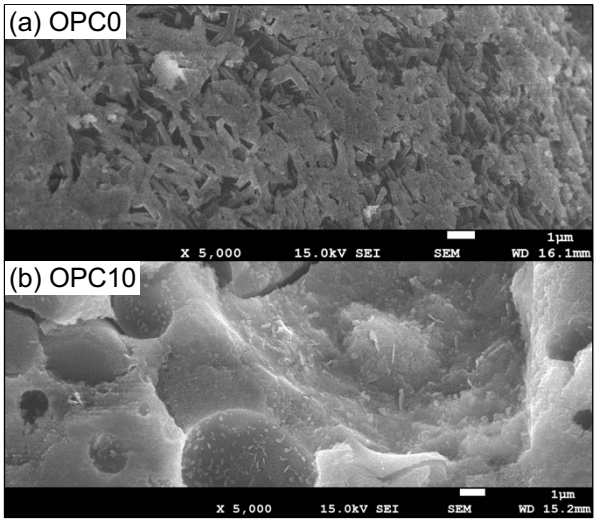

Fig. 4 SEM micrographs of 28-day cured geopolymer mortar

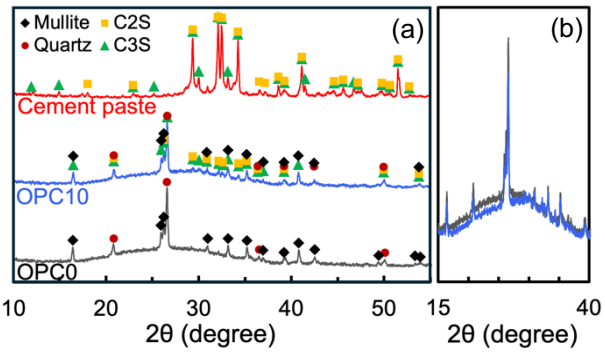

Fig. 5 XRD analysis

in the reaction products, which aligns with the SEM observations. Furthermore, it has been reported that crystalline peaks associated with $Ca(OH)_2$ are absent in XRD analysis, suggesting the formation of amorphous rather than crystalline $Ca(OH)_2$ [7]. Similarly, crystalline $Ca(OH)_2$, which has a distinctive hexagonal prism morphology, was not observed in the SEM micrographs obtained in this study. Moreover, Nakamura et al. suggested that, under high alkaline environment such as that found in geopolymer, ettringite is unstable and rapidly decomposes, restructuring into Na-typed monosulfoaluminate [8]. This explains the absence of ettringite in the reaction products of OPC10. Fig. 5(a) presents the XRD analysis results, which only detected mullite, quartz, tricalcium silicate (C_3S) and dicalcium silicate (C_2S) in OPC10. Taking into account that only 10% cement was added, the typical crystalline hydration products, namely $Ca(OH)_2$ and ettringite, might be difficult to be found within the products of geopolymer with cement added. From the analysis of the cement paste, it is clear that beside C_3S and C_2S, the typical crystalline cement hydration products were not detected, suggesting that under high alkaline environment, cement hydration takes place in a manner that produces distinct reaction products. This may lead to the absence of the typical crystalline products or extremely low amount that is undetectable by the XRD analysis, which is consistent with the previous studies.

While the high alkalinity of geopolymer

compromised the cement hydration process, the resulting cement hydration also exerted a reverse effect on the hardening reaction of geopolymer. To understand the influence of cement hydration on geopolymerization, it is essential to first comprehend the reaction mechanism of geopolymer. According to the JSCE [4], the hardening mechanism of geopolymer can be divided into two main processes, the breakdown of the starting materials and the formation of the reaction products. Under the action of hydroxide ions in the alkaline solution, silicate and aluminate ions dissolve from fly ash. Along with the silicate ions already present in sodium silicate, these ions undergo dehydration, polymerization, and condensation to form the reaction products. It is important to highlight that although water is not consumed throughout the hardening process of geopolymer, the dissolution of the starting materials can only take place in the presence of water. Therefore, water is required to initiate the hardening of geopolymer.

Since the precipitation of $Ca(OH)_2$ proceeds at an unprecedented rate when cement is added, it results in a rapid water consumption in the mixture during the early stages of the hardening process. Given the critical role of water in the hardening of geopolymer, it is believed that the rapid water loss in the fresh geopolymer mixture may hinder the dissolution of the fly ash. As displayed in Fig. 4(b), traces of unreacted fly ash are still present. This results in a reduced number of monomers, a lower degree of polymerization, and weaker geopolymer frameworks. The XRD analysis results presented in Fig. 5(b) further supports this observation. Comparing OPC0 and OPC10, a broad intensity bump is observed between 15 and 40 degrees, which is believed to express the intensity of the amorphous geopolymer gel. The smaller bump area in OPC10 suggests a reduced amount of geopolymerization products. This reduction corroborates the hypothesis that cement addition decreases geopolymerization efficiency due to rapid water consumption and hindered fly ash dissolution.

The mutual influence of cement and geopolymer compromises the reaction products of both cement hydration and geopolymerization process, particularly leading to the absence of the typical cement hydration products and simultaneously inducing structural modification in geopolymer, resulting in a less pronounced columnar structure. Consequently, the overall compressive strength of the cement-incorporated geopolymer mortar is lower than that of the geopolymer mortar without cement, due to the dominance of geopolymer reaction products within the cement-geopolymer system.

3.2 Pore Size Distribution

It has been suggested that pore size could be a pivotal component in determining the magnitude of shrinkage [9]. Therefore, the change in pore size distribution due to cement addition is discussed here. Fig. 6 and Fig. 7 demonstrate the pore size distribution of the geopolymer mortar cured for 3 and 28 days, respectively. The solid lines represent the pore volume at each pore diameter, while the dotted lines denote the cumulative pore volume. With the incorporation of cement, the peak pore volume shifted from locating at a diameter of approximately 0.016μm to 0.014μm for 3-day cured specimen and 0.013μm to 0.009μm for 28-day cured specimen, suggesting increases in the number of smaller pores. However, no significant difference was observed in the total pore volume measured by MIP.

Mehta and Monteiro [10] have classified capillary voids into two types based on their sizes. Capillary voids smaller than 0.05μm are referred to as “micropores”, while those larger than 0.05μm are referred to as “macropores”. The removal of water held by capillary tension in the micropores (0.005μm ~ 0.05μm), is the driving force of drying shrinkage. On the other hands, macropores, whose water removal does not cause volume change, are more influential in determining the strength of the material. Table 3 lists the volumes of micropores and macropores of the geopolymer mortar with and without cement addition. $\Delta V/V_0$ indicates the change in the volume of each type of pore after cement addition. It can be inferred that, regardless of the curing period, mixing cement with geopolymer reduces the total volume of micropores and increases the total volume of macropores.

Ng et al. concluded in their study that the enhancement of geopolymerization blocks the interconnectivity between pores, which leads to a denser geopolymer matrix with higher compressive strength [11]. Building on the assumption that rapid cement hydration results in a lower degree of polymerization, the number of pores of the reaction products increases, which is reflected in the growth of the macropore volume in geopolymer upon cement addition. Furthermore, since

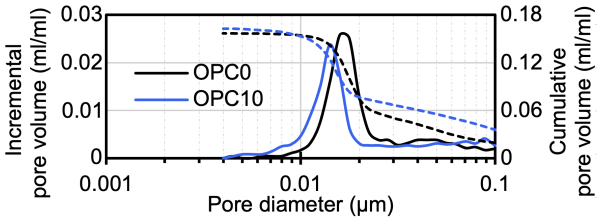

Fig. 6 Pore size distribution of 3-day cured geopolymer mortar

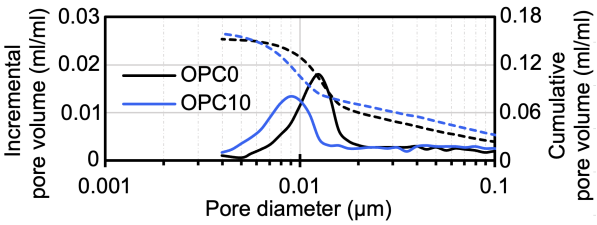

Fig. 7 Pore size distribution of 28-day cured geopolymer mortar

Table 3 Micropore and macropore volumes

Curing period	OPC (%)	Micropores		Macropores	
		Volume	$\Delta V/V_0$	Volume	$\Delta V/V_0$
3 days	0	0.125		0.032	
	10	0.110	-12%	0.051	59%
28 days	0	0.116		0.035	
	10	0.109	- 6%	0.046	31%

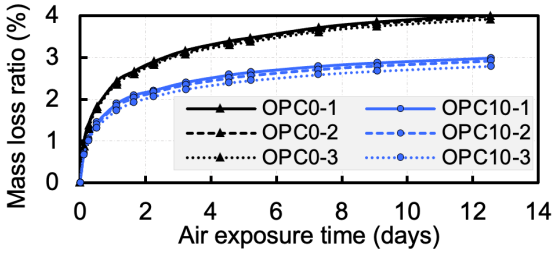

Fig. 8 Mass loss ratio of 3-day cured geopolymer mortar

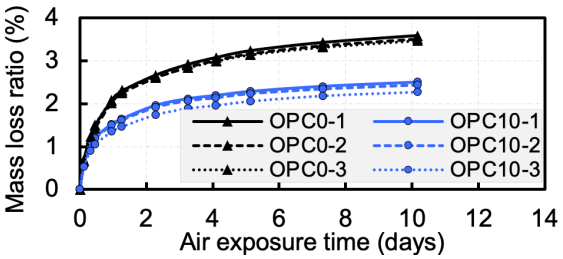

Fig. 9 Mass loss ratio of 28-day cured geopolymer mortar

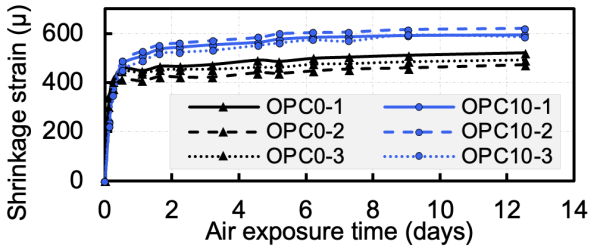

Fig. 10 Shrinkage strain of 3-day cured geopolymer mortar

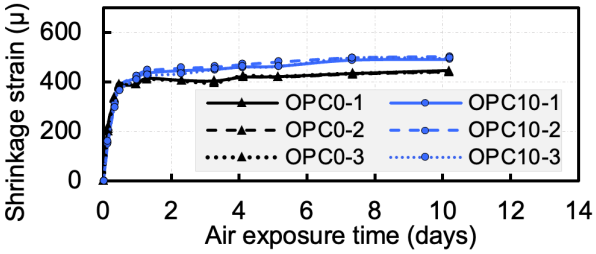

Fig. 11 Shrinkage strain of 28-day cured geopolymer mortar

the macropores are strongly correlated with the strength of the material, this finding aligns with the experimental results in this study, which shows that cement incorporation increases the number of macropores and decreases the compressive strength.

On the other hand, the decreases in the micropores are attributed to the shift in the peak of the pore size distributions. As the pores size becomes more concentrated in smaller diameters within micropore range, it consequently results in a lower accumulated volume. Due to the limitations of the analytical equipment, it was not possible to visualize the pore structure at the nanoscale or confirm its relationship with the pore size distribution. Although the underlying mechanism remains unclear, it is evident that the transitions in the pore size distribution result from the addition of cement.

3.3 Mass Loss Ratio and Drying Shrinkage Strain

Fig. 8 and Fig. 9 show the mass loss ratio of geopolymer mortar cured for 3 and 28 days, respectively. The numbers following the hyphen (1, 2, 3) denote each of the three specimens in each case. For both curing periods, OPC10 shows a lower mass loss ratio compared to OPC0, indicating that specimens with cement added experienced a lower level of water evaporation. For instance, after seven days of air exposure, the water evaporation dropped by 27% and 32% for geopolymer mortar cured for 3 and 28 days, respectively, upon the addition of cement.

In discussing moisture retention within a hardened cementitious material and moisture transport between the pores of the reaction products and the surrounding environment due to the changes in relative humidity, Maekawa et al. [12] explained that, from a microscopic perspective, the pressure difference between the liquid-vapor phases would be balanced by the curved vapor-liquid interfaces (meniscus) formed in the numerous pores of the microstructure. The continuity of the stress field across such interfaces is modified by the surface tension, which contributes to the formation of capillary tension. In the equilibrium state, Maekawa et al. obtained r_s (the largest radius of the pores where water can be stably retained) from the Kelvin's equation which can be expressed as follows:

$$r_s = -\frac{2\gamma M}{\rho R T}\frac{1}{\ln h} \quad (1)$$

where,

γ :surface tension
M :molecular weight
ρ :water density
R :universal gas constant
T :temperature
h :relative humidity

By integrating the pore volume lying below r_s, expression of water content remained in the pores can be calculated. In order words, the amount of water evaporation at any given h can also be estimated. Under the same humidity condition, both OPC0 and OPC10 shared the same r_s value, as parameters such as γ, M, ρ, R, and T remain constant. Consequently, it is the pore size distribution that distinguishes the water content, as it defines the pore volume function used in the integration. Since the pore size distribution of OPC10 is more concentrated at smaller diameters compared to that of OPC0, the water content retained in pores of radii smaller than r_s at a relative humidity of 60% is higher for OPC10. This leads to a lower mass loss due to water evaporation for OPC10.

Fig. 10 and Fig. 11 show the shrinkage strain of the 3-day and 28-day sealed cured geopolymer mortar, respectively. The numbers following the hyphen (1, 2, 3) denote each of the three specimens in each case. Regardless of the curing period, the shrinkage strain increases at an identical rate during the first 10 hours of air exposure for both OPC0 and OPC10. However,

beyond this period, the rate of increase in shrinkage strain of OPC0 begins to decelerate rapidly. In contrast, the shrinkage strain of OPC10 continues to progress at a higher rate, eventually resulting in a greater shrinkage for OPC10 after prolonged air exposure. For example, after seven days of being exposed to a 60%R.H. environment, the shrinkage strain increased by 23% and 14% for 3-day and 28-day cured geopolymer mortar, respectively, upon cement addition.

Shimomura and Maekawa [13] observed that capillary tensile forces set up at the meniscus are intensified as the radius of the pores where the meniscus forms get smaller, thereby increasing the shrinkage. This suggests that within the range of micropores, where water removal correlates the volume change, smaller pores exert a greater influence on drying shrinkage than larger ones. Given the higher volume of smaller pores in OPC10, it can be inferred that the cement addition induces greater capillary tensile forces, leading to more pronounced drying shrinkage. In contrast, geopolymer mortar without cement exhibits smaller and faster-converging drying shrinkage due to its lower volume of smaller pores.

In addition to the role of micropores in drying shrinkage, changes in macropore volume also influence shrinkage behavior, even though they do not directly determine the magnitude of the drying shrinkage. As previously discussed, the volume of macropores is strongly linked to the degree of hardening reaction as well as the strength of the material. Specifically, a higher volume of macropores corresponds to weaker material strength, as the progression of hardening reaction reduces macropores and enhances the material strength [10,11]. According to Mehta and Monteiro [10], the existence of the van der Waals forces of attraction is the principal source of strength in the solid products of the hydrated cement paste, with adhesion between solid surfaces attributed to these physical forces. Assuming that the same principle of attraction applies to hardened geopolymeric material, its strength can be associated with attraction forces that contribute to the material's resistance to deformation. Based on the hypothesis that cement incorporation into geopolymer mortar induces rapid cement hydration, which results in an increased volume of macropores and a lower degree of geopolymerization, the reduction in compressive strength due to cement addition weakens adhesion between the reaction products. Consequently, this makes the geopolymer mortar less resistant to drying shrinkage.

4. CONCLUSIONS

This study examined the coexistence of geopolymerization and cement hydration by incorporating a small portion of cement into geopolymer mortar and evaluating its drying shrinkage behavior. The findings revealed that the high alkalinity of the geopolymer solution caused rapid cement hydration, which disrupted geopolymerization, resulting in structural modifications of the reaction products. The change in pore size distribution is believed to result in larger capillary tensile forces and reduced material strength, thereby intensifying the magnitude of drying shrinkage and lowering the material resistance to drying shrinkage, respectively.

REFERENCES

[1] Ichimiya, K., Hatanaka, S. and Atarashi, D., "Current Status and Future Prospects of Geopolymer," Concrete Journal, Vol. 56, No. 5, May 2018, pp. 409-414. (In Japanese)

[2] Ichimiya, K. et al, "Study on Geopolymer Resistance to Acid and Alkali Silica Reaction," Research Presentation Meeting of the Western Branch of the JSCE, Mar. 2011, pp. 687-688. (In Japanese)

[3] Ikeda, K., "Consolidation of Mineral Powders by the Geopolymer Binder Technique for Materials Use," Shigen-to-Sozai, Vol. 114, 1998, pp. 487-500.

[4] JSCE, "Report on the Achievements of the Research Subcommittee for Promoting the Practical Application of Geopolymer Technology in the Civil Engineering Field Concrete Engineering Series, No.132, 2022. (In Japanese)

[5] Jawed, I. and Skalny, J., "Akalies in Cement: A Review. II. Effects of Alkalies on Hydration and Performance of Portland Cement," Cement and Concrete Research, Vol. 8, 1978, pp. 37-52.

[6] Phair, J. W., van Deventer, J. S. J. and Smit, J. D., "Mechanism of Polysialation in the Incorporation of Zirconia into Fly Ash-Based Geopolymers," Industrial & Engineering Chemistry Research, Vol. 39, No. 8, 2000, pp. 2925-2934.

[7] Yip, C. K., Lukey, G. C. and van Deventer, J. S. J., "The Coexistence of Geopolymeric Gel and Calcium Silicate Hydrate at the Early Stage of Alkaline Activation, Cement and Concrete Research, Vol. 35, 2005, pp. 1688-1697.

[8] Nakamura, S. et al, "Study on Hydration of Expansive Agent in Geopolymer, Proceedings of the JCI, Vol. 40, No. 1, 2018, pp. 1833-1838. (In Japanese)

[9] Collins, F. and Sanjayan, J. G., "Effect of Pore Size Distribution on Drying Shrinkage of Alkali-Activated Slag Concrete, Cement and Concrete Research, Vol. 30, 2000, pp. 1401-1406.

[10] Mehta, P. K. and Monteiro, P. J. M., "Concrete – Microstructure, Properties, and Materials," McGraw-Hill, 2006, pp. 29-44.

[11] Ng, C. et al, "A Review on Microstructural Study and Compressive Strength of geopolymer Mortar, Paste and Concrete," Construction and Building Materials, Vol. 186, 2018, pp. 550-576.

[12] Maekawa, K., Ishida, T. and Kishi, T., "Multi-scale Modeling of Structural Concrete," Taylor & Francis, 2009, pp. 132-133.

[13] Shimomura, T. and Maekawa, K., "Analysis of the Drying Shrinkage Behavior of Concrete Based on the Microscope Structure of the Concrete using a Micromechanical Model," Magazine of Concrete Research, Vol. 49, No. 181, 1997, pp. 302-322.